Technical Paper

Sorption-desorption column tests to evaluate the attenuation layer using soil amended with a stabilising agent

Tomohiro Kato [a],[*], Lincoln W. Gathuka [a], Takaomi Okada [a], Atsushi Takai [a]
Takeshi Katsumi [a], Yukari Imoto [b], Kazuya Morimoto [b], Miu Nishikata [b], Tetsuo Yasutaka [b]

[a] *Graduate School of Global Environmental Studies, Kyoto University, Yoshida-honmachi, Sakyo-ku, Kyoto 606-8501, Japan*
[b] *National Institute of Advanced Industrial Science and Technology, 1-1-1 Higashi, Tsukuba, Ibaraki 305-8567, Japan*

Abstract

Sorption-desorption column tests using acrylic columns (ϕ 5 cm $\times$ h 10 cm) were employed to evaluate the sorption performance of an attenuation layer against geogenic contamination. The attenuation layer material was silica sand amended with 1, 5, or 10% of a stabilising agent. The main component of the agent was magnesium oxide. The sorption behaviour of the materials was determined by a fluoride solution ($C_0 = 80$ mg/L F$^-$), while the desorption behaviour was determined by distilled water. Breakthroughs ($C/C_0 > 0.05$) occurred after approximately 1, 20, and 50 PVF for stabilising agent contents of 1, 5, and 10%, respectively. The one-dimensional advection-dispersion equation modelled the breakthrough curves obtained from the tests. The predictions gave unrealistic estimates, especially for the breakthrough point where $C/C_0 = 0.05$. For the 1% agent content, approximately 20% of the sorbed mass, S_s, was desorbed, but the percentage of desorbed mass, S_d, was much smaller for the higher agent contents. The difference between the sorbed and desorbed masses was defined as the immobilised fraction, $S_s - S_d$. For the 5% agent content, $S_s - S_d = 4.0$ mg/g. The results suggest that when silica sand is amended with magnesium oxide as an agent, the mixture can immobilise the fluoride in the attenuation layer.
© 2021 Production and hosting by Elsevier B.V. on behalf of The Japanese Geotechnical Society. This is an open access article under the CC BY-NC-ND license (http://creativecommons.org/licenses/by-nc-nd/4.0/).

Keywords: Fluoride; Geogenic contamination; Magnesium oxide; Partition coefficient; Advection-dispersion analysis

1. Introduction

To reduce the disposal of soils, the excavation of new materials, the carbon footprint, etc., the utilisation of soils and rocks excavated at construction sites is highly encouraged (e.g., Magnusson et al., 2019). However, the utilisation of these materials in Japan remains a challenge for several reasons. One big concern is that a certain percentage of these excavated materials contain toxic geogenic chemicals, such as arsenic (As), fluorine (F), and lead (Pb) (e.g., Naka et al., 2016; Tabelin et al., 2018; Tamoto et al., 2015). If contaminated materials fail to meet the environmental standards and/or the Soil Contamination Countermeasures Law (SCCL), actions for contaminant control must be implemented (e.g., Katsumi et al., 2019; Ministry of Land, Infrastructure, and Transport, 2010). Considering the leaching load and the nature of the materials, measures such as containment and chemical treatment are inappropriate for two main reasons. First of all, in many cases, toxic chemicals are leached in concentrations that slightly exceed the mandated limits under the SCCL (e.g., Ito and Katsumi, 2020). Second of all, although significantly large volumes of excavated soils and rocks are generated at construction sites, only a certain percentage contains toxic chemicals (e.g., Ministry of Land, Infrastructure, and Transport, 2010). Therefore,

---

the implementation of cost-effective countermeasures for the proper utilisation of these contaminated materials is desirable (Katsumi, 2015).

One possible countermeasure for preventing the contamination of the adjacent ground, where such contaminated soils are utilised, is the attenuation layer method. The benefits of this method are its low material costs and reduced management efforts (e.g., Tatsuhara et al., 2012, 2015; Nozaki et al., 2013a). To prevent (or reduce to acceptable levels) the infiltration of toxic chemicals from these contaminated materials into the adjacent ground, an attenuation layer is installed on the embankment foundation, as shown in Fig. 1 (Mo et al., 2020; Nozaki et al., 2013b; Tabelin et al., 2013). A typical attenuation layer material is clean sandy soil mixed with a stabilising agent.

The sorption performance should be evaluated for the attenuation layer to prevent the infiltration of contaminants. The partition coefficient, K_d (cm^3/g), is a common index for evaluating the sorption performance of geomaterials. This parameter can be determined through various laboratory experiments, including batch tests, column tests, and other experimental methods. The advantage of the batch test is that it has a simple experimental protocol with a short testing time. In this test, K_d is obtained from at least one of the empirical sorption isotherms. However, the applicability of this test is limited for three reasons. Firstly, it usually employs a liquid-to-solid (L/S) ratio of 10–50 L/kg, which is much higher than the in-field infiltration. Secondly, it is difficult to distinguish the temporal changes in concentrations (Martínez-Lladó et al., 2011). Thirdly, the test does not consider solute kinetics or the in-field flow conditions (Plassard et al., 2000).

Recently, the column test has become more prevalent for evaluating the sorption performance. In this test, the concentrations in the effluents can be monitored for several L/S ratios, including much smaller ratios than in the batch test. The smaller L/S ratios can better represent the in-field conditions. By modelling the breakthrough curves from this test, K_d can be determined (Igarashi and Shimogaki, 1998; Martínez-Lladó et al., 2011; Wang and Liu, 2005).

The sorption performance of the stabilising agent against geogenic contaminants is more commonly investigated by batch experiments (e.g., Morishita and Wada, 2013; Nishikata et al., 2020; Nozaki et al., 2013b) than by column experiments (Mo et al., 2020; Tatsuhara et al., 2012). Furthermore, the sorption performance of the agent

has been individually evaluated (Nishikata et al., 2020; Nozaki et al., 2013b; Tabelin et al., 2013), while the soil-agent mixture has not been fully evaluated. As an evaluation of the sorption performance closer to the in-field conditions, it should be performed by column tests using a soil-agent mixture.

Contaminants sorbed by a soil-agent mixture should be immobilised in the attenuation layer. The concentrations of geogenic contaminants leached from excavated soils often decrease and approach zero over time (Inui et al., 2014; Naka et al., 2016). In this situation, contaminants sorbed by relatively weak chemical interactions may be desorbed by seepage water. The desorption behaviour should be considered in order to evaluate the sorption performance of the attenuation layer.

Sorption-desorption column tests have the potential for use in evaluating the attenuation layer. This test has been conducted to assess 1) the migration characteristics of chemicals in the ground (Igarashi and Shimogaki, 1998; Wang and Liu, 2005), 2) the recovery percentage of metals in soils (Martínez-Lladó et al., 2011), and 3) the regeneration of the sorption performance (Ye et al., 2018). The sorption-desorption column test can indicate whether contaminants immobilised by soil amended with a stabilising agent are leached during the desorption phase because weakly attracted contaminants can be leached.

In this study, sorption–desorption column tests were conducted to discuss the sorption performance of soil amended with a stabilising agent. Fluoride (F$^-$) was selected as the target contaminant because it is a geogenic contaminant whose concentration exceeds the acceptable limit regulated under the SCCL (e.g., Ito and Katsumi, 2020; Naka et al., 2016). Magnesium oxide (MgO) was used as the stabilising agent because it is a promising agent for the attenuation layer (Wada and Morishita, 2013; Nozaki et al., 2013b). To estimate the sorption and desorption parameters, the analytical solution for the one-dimensional advection-dispersion equation (ADE) was fitted to the breakthrough curves obtained from column experiments.

2. Materials and methodologies

2.1. Materials

Silica sand was used as the clean parent material. Table 1 summarises its physical properties. Fig. 2 shows its X-ray
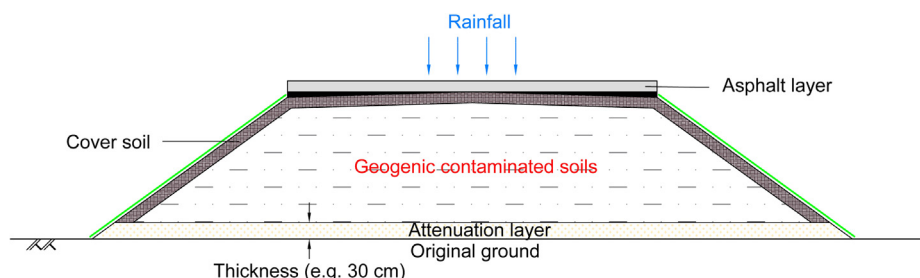

Fig. 1. Schematic of conventional design of attenuation layer method.

diffraction (XRD) profile with CuKα, 40 kV, 100 mA (RINT-2500, Rigaku in GSJ-Lab, AIST).

The stabilising agent was manufactured by Taiheiyo Cement. The chemical composition of the agent was evaluated by X-ray fluorescence (XRF) (EDX-720, Shimadzu), and it was determined that the agent mainly constituted MgO and its content was ~91%. It also contained a certain amount of CaO (~6.7%). It had a Blaine specific surface area of 5970 cm^2/g, which was determined as per JIS R 5201 (2015). The residue on a 90-μm sieve was 21.2 wt%. It had a particle density of 3.21 g/cm^3, which was determined as per JIS R 5201 (2015).

The test specimens had three agent contents (1, 5, or 10%). These agent contents of 1, 5, and 10% corresponded to stabilising agent contents of 10 g-, 50 g-, and 100 g per kg of dry soil, respectively. In the experiment, silica sand was poured into a steel bowl, and then the appropriate amount of stabilising agent was added. Finally, the sand and the stabilising agent were manually mixed with care to prepare the homogenous mixtures.

2.2. X-ray diffraction analysis

2.2.1. Hydration tests

Understanding hydration kinetics is important for evaluating the sorption performance of MgO. Here, hydration tests were used to investigate whether hydration was complete within 24 h. In these tests, 0.6-g samples of the agent were put in contact with 30 mL of distilled water using plastic tubes. To investigate the kinetics of hydration as fundamental information, the samples were left for a given length of time (1, 4, or 27 days). After the hydration tests, the solid and the liquid were separated using centrifugation. The pH values of the liquid were measured using a pH/EC meter (F-54, Horiba). The XRD profiles with CuKα, 40 kV, 100 mA were measured after 1, 4, and 27 days.

2.2.2. XRD pattern for sample after column tests

An XRD analysis was conducted after completing the sorption–desorption column test for a 10% agent content. It took 110 days to complete the column test for a 10% agent content. The agent particles were manually separated from the particles of silica sand after freeze-drying with a freeze dryer (FDS-1000, EYELA). The freeze-dried specimen was sieved by passing it through a 106-μm opening
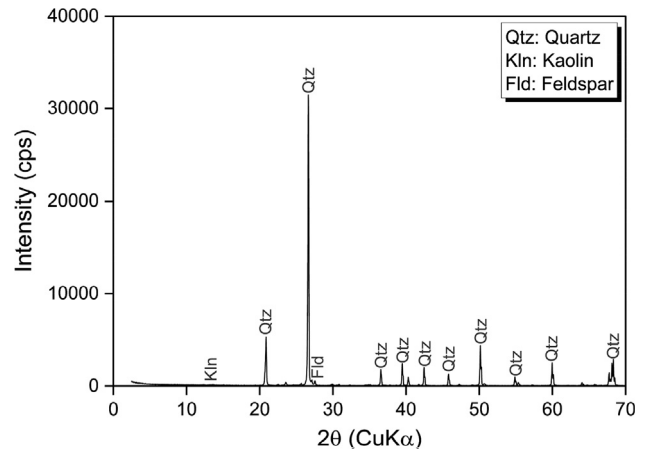

Fig. 2. XRD profile of the silica sand.

screen. Afterwards, the sieved material was examined by XRD analysis. Only the 10% case was evaluated because it was difficult to distinguish the agent particles from the silica sand. Even at this relatively high agent content, the sieving step could not remove all the quartz particles. However, the passing fraction was mainly considered to show the components of the agent particles after the column test.

2.3. Sorption-desorption column tests

Sorption-desorption column tests were used to evaluate the sorption and desorption behaviours of the specimens. Two-stage column tests were conducted using acrylic columns (ϕ 5 cm × h 10 cm) at room temperature (~20 °C). A dried soil-agent mixture was placed in the column. Each specimen was compacted in the acrylic column in five layers of equal heights. During compaction, a 125-g rammer was dropped freely from a height of 20 cm. This method was based on the corresponding ISO 21268-3 (2019). The specimen was placed between filter papers to prevent channel clogging due to the fine soil particles. Then distilled water was percolated in an up-flow direction using a peristaltic pump at a flow rate of approximately 36 mL/h until the specimen reached saturation. Finally, percolation was interrupted for 24 h to achieve a saturated condition. Table 2 summarises the test conditions. Side wall leakage should not occur in this test considering two aspects. The first aspect is that the hydraulic conductivity of this silica sand is approximately 10^{-4} m/s ~ 10^{-5} m/s. The second aspect is that the ratio of the maximum particle size to the column diameter is less than 1/40.

Table 1
Physical properties of silica sand.

Parameter	Standard	Value
Particle density	JIS A 1202 (2009)	2.62 g/cm^3
Particle size distribution	JIS A 1204 (2009)	
Sand [0.075–2 mm]		98%
Fines [<0.075 mm]		2%
Maximum particle size		0.425 mm
Coefficient of uniformity		1.04
Coefficient of curvature		2.17

Table 2
Specimen properties used in this study.

Agent content (%)	ρ_d (g/cm³)	n
1	1.40	0.47
5	1.38	0.48
10	1.43	0.47

In the first stage (sorption phase), the influent was a fluoride solution prepared using sodium fluoride (NaF) with a concentration of $C_0 = 80$ mg/L F⁻. The solution was continuously percolated in an up-flow direction via a peristaltic pump at 36 mL/h, which is equivalent to a Darcian velocity of 44 cm/d. The first stage was terminated when the concentration in the effluent, C, exceeded 76 mg/L F⁻, where $C/C_0 = 0.95$. In the second stage (desorption phase), distilled water was percolated under the same flow conditions until the concentration in the effluent was less than 4 mg/L F⁻, where $C/C_0 = 0.05$.

Effluents were collected periodically in plastic bottles and filtered using a 0.45-µm membrane filter. The filtrate pH was measured using a pH/EC meter (F-54, Horiba). The fluoride concentration was measured using a fluoride selective electrode (6561S-10C, Horiba).

2.4. Solute transport analysis

2.4.1. Theory

Breakthrough curves from the column tests can be modelled using a one-dimensional ADE as

$$R\frac{\partial C}{\partial t} = D\frac{\partial^2 C}{\partial x^2} - v\frac{\partial C}{\partial x} \qquad (1)$$

Assuming that the initial and 'constant-flux' boundary conditions are given as

$$C|_{x \geqslant 0, t=0} = 0, \; -D\frac{\partial C}{\partial x} + vC\Big|_{x=0, t \geqslant 0} = vC_0, \frac{\partial C}{\partial x}\Big|_{x=\infty, t \geqslant 0}$$
$$= 0 \qquad (2)$$

the solution to Eq. (1) for these conditions is given by van Genuchten and Parker (1984) as

$$\frac{C}{C_0} = \tfrac{1}{2}\mathrm{erfc}\left[\frac{RL-vt}{(4RDt)^{1/2}}\right] + \left(\frac{v^2 t}{\pi RD}\right)^{1/2}\exp\left[-\frac{(RL-vt)^2}{4RDt}\right]$$
$$-\tfrac{1}{2}\left(1 + \frac{vL}{D} + \frac{v^2 t}{RD}\right)\exp\left(\frac{vL}{D}\right)\mathrm{erfc}\left[\frac{RL+vt}{(4RDt)^{1/2}}\right] \qquad (3)$$

where R ($= 1 + \rho_d K_d/n$, in which ρ_d (g/cm³) and n are the dry density and porosity of the specimen, respectively) is the retardation factor, D (cm²/s) is the longitudinal dispersion coefficient, v (cm/s) is the average pore water velocity, C (mg/L) is the solute concentration at distance x from the source at time t, C_0 (mg/L) is the initial solute concentration, and L (cm) is the column length.

To model the breakthrough curves from the tests, it is assumed that the solute transport parameters, R, D, v, and C_0, are constant. For the sorption phase, the experimental data were directly fitted using Eq. (3). For the desorption phase, the experimental data were fitted using Eq. (3), but C/C_0 was subtracted from 1 [i.e. $(1 - C/C_0)$], as recommended by Grathwohl and Susset (2009). This is because the initial and boundary conditions for the desorption phase differ from those of the sorption phase, as shown in Fig. 3.

2.4.2. Estimation of D values using chloride tracer tests

Tracer tests were conducted to determine the values for D during the sorption and desorption phases after the sorption–desorption column tests. This test followed the two-stage column test using the same specimen (Table 2). Chloride (Cl⁻) was used as the non-sorbed chemical. A chloride solution with a concentration of 1000 mg/L Cl⁻ was prepared using sodium chloride (NaCl). The specimens were percolated using the Cl⁻ solution until the concentrations in the effluents were 1000 mg/L Cl⁻, where $C/C_0 = 1.0$. After that, percolation was continued using distilled water until the concentrations in the effluents were 50 mg/L Cl⁻, where $C/C_0 = 0.05$. The flow rate was similar to that in the two-stage column tests (refer to Section 2.3). The chloride concentration was measured using a chloride selective electrode (6560S-10C, Horiba).

To estimate the values for D, the breakthrough curves were modelled from the tracer test using Eq. (3). As Cl⁻ is a non-sorbed chemical, it was assumed that $R = 1$. The values for D were obtained by minimising the residual sum of the squares (SSE) between the predicted data and the experimental data as

$$\mathrm{SSE} = \sum_{i=1}^{n}\left[(C/C_0)_i - (C/C_0)'_i\right]^2 \qquad (4)$$
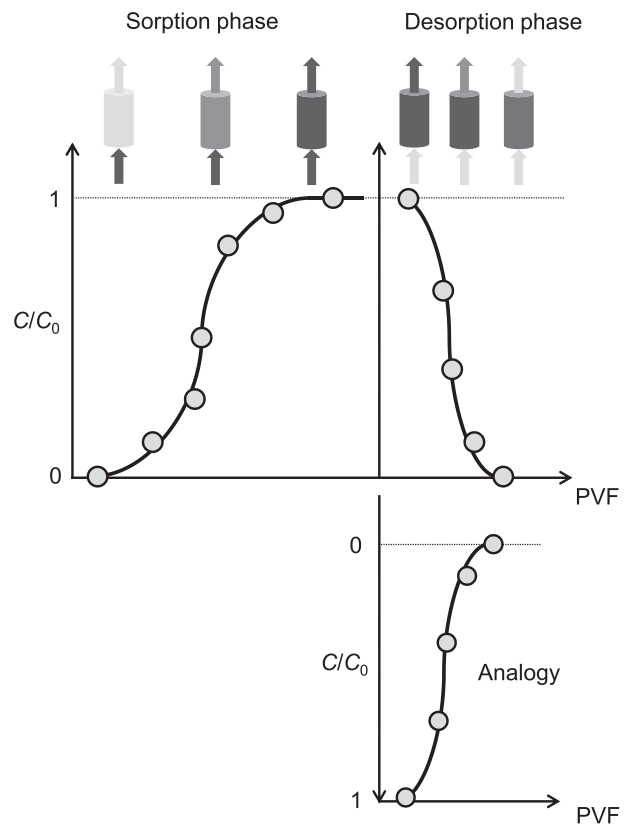

Fig. 3. Parameter determination in an analytical solution, where the sorption and desorption phases are determined using the results of the column test and analogical concept, respectively.

where $(C/C_0)_i$ is the experiment data series and $(C/C_0)_i'$ is the predicted data series. When the experimental value and the analytical solution at $C/C_0 = 0.5$ disagreed, the v value in the analytical solution was manually adjusted.

Fig. 4 and Table 3 summarise the results of the tracer tests. The obtained prediction curves are analogous to the experimental data.
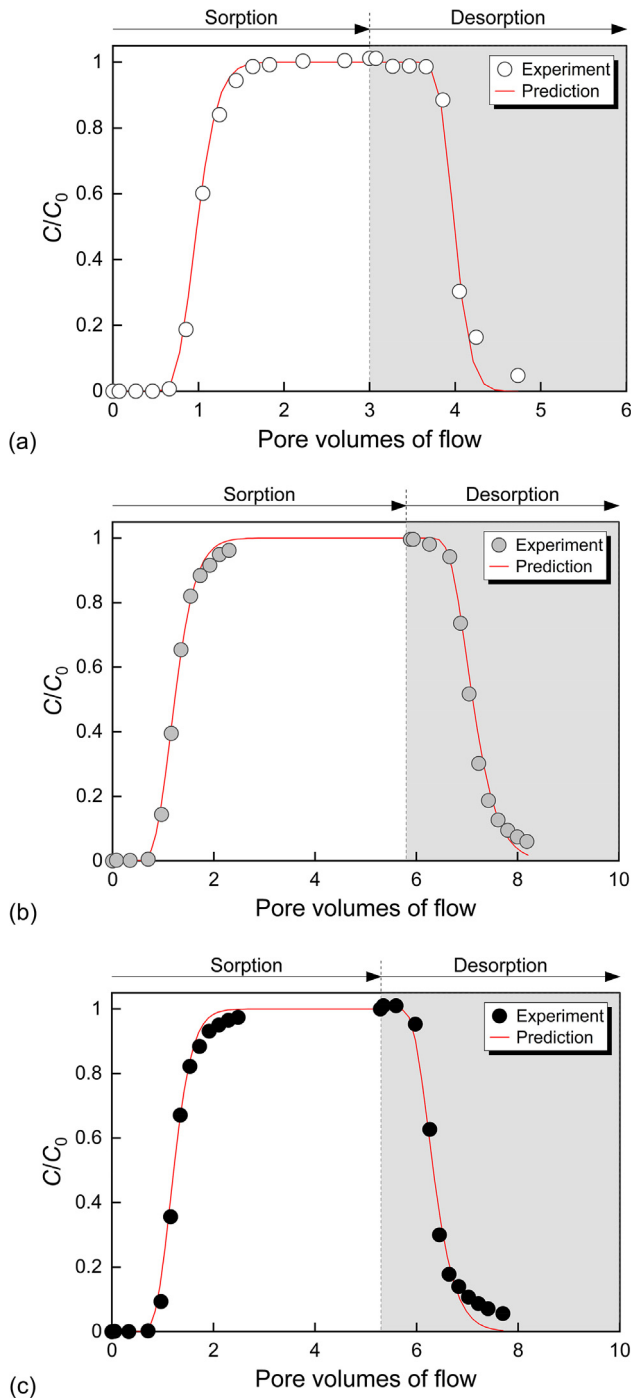
2.4.3. Determination of partition coefficients

The values for R were determined using the D values obtained from Section 2.4.2 and minimising the error between the predicted data and those from the two-stage column tests. Then the values for K_d were calculated from the obtained R. Although R can be used as an index, K_d is more commonly used when designing geochemical barrier systems in Japan.

3. Results

3.1. Hydration kinetics

The hydration kinetics of the stabilising agent was investigated based on Section 2.2.1. Fig. 5(a) shows the XRD patterns. Prior to hydration, the MgO peaks were significant, but during hydration, the magnesium hydroxide [Mg(OH)$_2$] peaks were predominant. However, the MgO peak was clearly observed after 27 days. These results show that the hydration kinetics of this agent is relatively slow, and that not all of the MgO was immediately hydrated after the 24-hour saturation step. Although this test did not consider or clarify the individual chemical reactions occurring in the column test, it did reveal the general trend of hydration kinetics. The pH values after 1, 4, and 27 days were 11.1, 11.7, and 9.89, respectively.

Fig. 5(b) shows the XRD pattern of the stabilising agent after the sorption-desorption column test. This XRD pattern was investigated based on the method described in Section 2.2.2. Peaks for both Mg(OH)$_2$ and MgO were detected. These results imply that the MgO contained in this agent is not consumed immediately. Quartz, kaolin, and feldspar peaks, derived from the silica sand component (refer to Fig. 2), were observed.

3.2. Sorption-desorption column tests

3.2.1. Transport parameters

Fig. 6 shows breakthrough curves obtained from the column tests. The changes in C/C_0 were evaluated with respect to the pore volumes of flow (PVF) during the sorption and desorption phases. The PVF was calculated by dividing the cumulative volume of the effluent collected during the test by the volume of the voids in the specimen. Previous research defined the breakthrough point as the concentration in the effluents where C exceeds 5% of C_0. That is, $C/C_0 = 0.05$ (Chen et al., 2011; Tor et al., 2009). Breakthroughs occurred after approximately 1, 20, and

Fig. 4. Results of the chloride tracer tests for agent contents of (a) 1%, (b) 5%, and (c) 10%.

Table 3
Solute transport parameters.

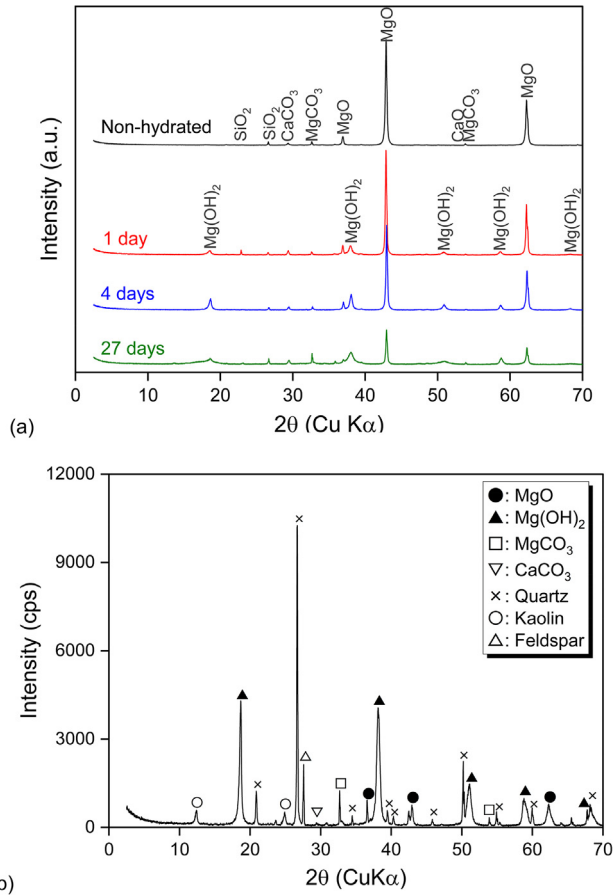| Agent content (%)	Sorption		Desorption	
	K_d (cm³/g)	D (cm²/s)	K_d (cm³/g)	D (cm²/s)
1	0.54	2.3×10^{-4}	0.081	1.3×10^{-4}
5	27	3.1×10^{-4}	0.13	4.3×10^{-4}
10	50	2.5×10^{-4}	0.11	5.4×10^{-4}

Fig. 5. XRD patterns of the stabilising agent (a) during hydration tests, and (b) after the column test.

50 PVF when using agent contents of 1, 5, and 10%, respectively. These results suggest that increasing the agent content can delay the breakthrough.

Table 3 summarises the values for K_d and D obtained during the sorption and desorption phases using the method described in Section 2.4. For the sorption phase, the prediction curve and the experimental data agreed relatively well, as shown in Fig. 6. However, the predictions gave different estimates for the breakthrough point ($C/C_0 = 0.05$). The predictions indicated that the breakthroughs occurred much later, namely, after approximately 2, 70, and 130 PVF for agent contents of 1, 5, and 10%, respectively. This means that the predicted retardation was not observed experimentally. Thus, the obtained K_d may not be a suitable index for evaluating the sorption performance. For the desorption phase, the predictions and the experimental data for $1 > C/C_0 > 0.4$ agreed well, but further modifications will be necessary to improve the agreement.

In terms of pH, all effluents were alkaline, as shown in Fig. 7. For an agent content of 1, 5, or 10%, the initial effluents had pH ~ 11.5. In all cases, the effluent pH decreased

as the number of PVFs increased. The pH > 11 values were higher than the expected values when $Mg(OH)_2$ was equilibrated with water. Although the reason is not completely clear, it is possible that this is because of the calcium. Fig. 5(a) shows that this stabilising agent contained some calcium oxide (CaO) and calcium carbonate ($CaCO_3$). Hence, it is possible that the Ca dissolved first, initially increasing the pH value to one higher than the Mg, and then the Mg dissolved slowly. In addition, the pH values during the hydration tests decreased after 27 days (refer to Section 3.1). The higher pH values might be attributed to the calcium contained in the stabilising agent. However, additional studies will be necessary to validate this assertion. Considering that the effluent pH was less than 12, as shown in Fig. 7, which is below the isoelectric points of MgO (=pH 12.4) and $Mg(OH)_2$ (=pH 12) (Parks, 1965), the net potential of the agent's surface should be positive. It is assumed that electrostatic attraction attracts fluoride on the surface.

3.2.2. Immobilised fraction

The immobilised fraction was calculated from the difference in the cumulative sorbed mass, S_s (mg/g), and the desorbed mass, S_d (mg/g) (i.e., S_s - S_d), using the obtained breakthrough curves shown in Fig. 8. $C/C_0 = 0.95$ is considered to be the exhaustion point for sorption; it implies that the sorbed fraction is almost saturated. On the other hand, $C/C_0 = 0.05$ is considered to be the exhaustion point for desorption; it implies that the desorbed fraction is almost saturated. S_s was calculated from the data on the sorption phase using Eq. (5), while S_d was determined from the data on the desorption phase using Eq. (6). For a better understanding and a clearer comparison, Fig. 8(b) plots S_s and S_d from 0 PVF. Cumulative fluoride sorbed mass S_s, per unit mass of soil-agent mixture, was calculated as follows:

$$S_s = \sum_{s=1}^{n} \frac{(C_0 - C_s)V_s}{m} \tag{5}$$

$$S_d = \sum_{d=1}^{n} \frac{C_d V_d}{m} \tag{6}$$

where C_s and C_d (mg/L) are the instantaneous effluent concentrations during the sorption and desorption phases, respectively, V_s and V_d (L) are the instantaneous volumes of the effluent collected during the sorption and desorption phases, respectively, and m (g) is the mass of the soil-agent mixture.

Fig. 9 shows the profiles of S_s and S_d for agent contents of 1, 5, and 10%. For agent contents of 1, 5 and 10%, S_s - S_d was estimated as 0.5, 4.0, and 6.0 mg/g, respectively. Considering the values for S_s and S_d, the desorbed amount was approximately 20% when using an agent content of 1%. A much smaller percentage of desorbed mass was estimated as the agent content increased.
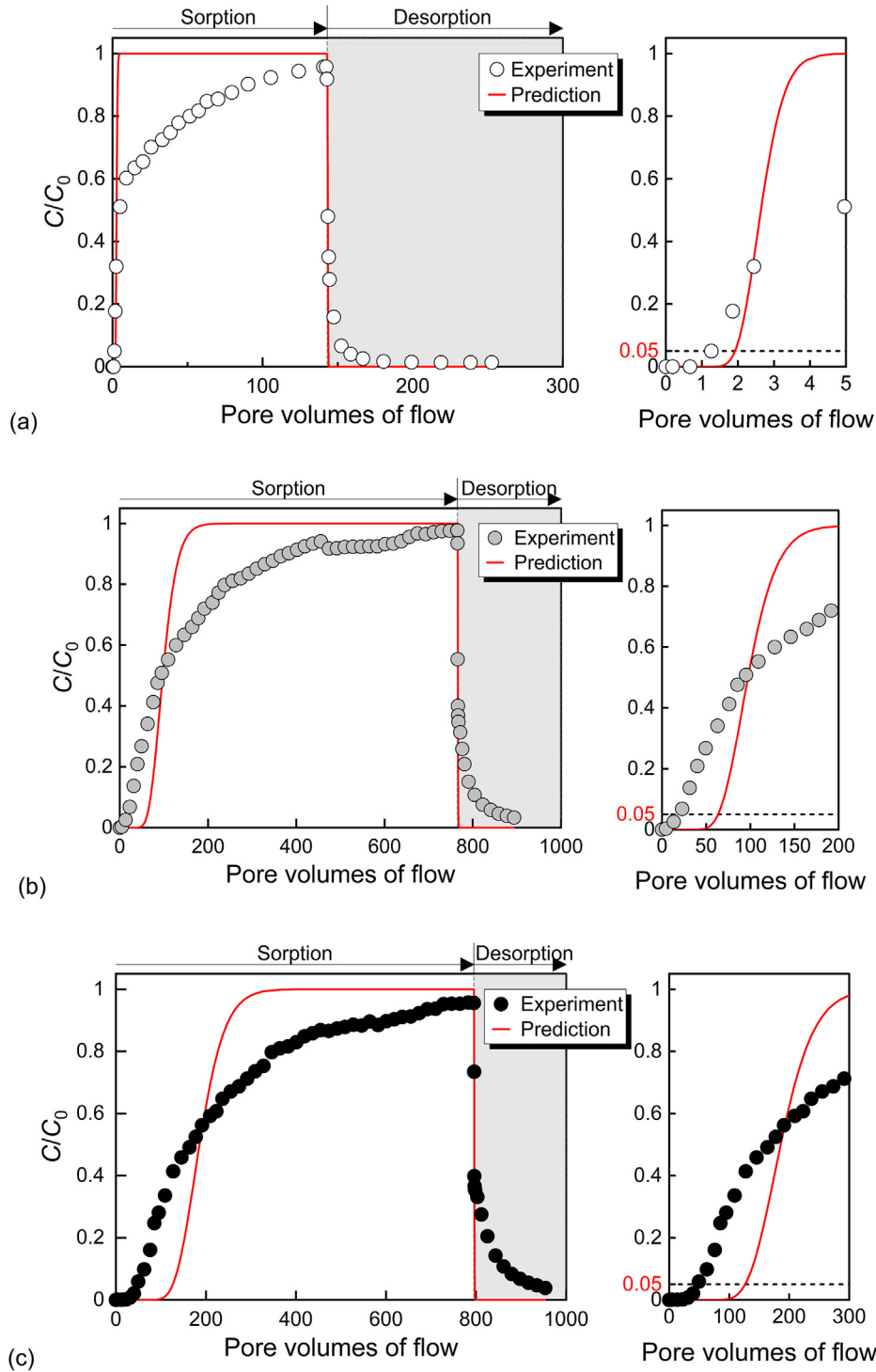
Fig. 6. Results of the sorption-desorption column tests for agent contents of (a) 1%, (b) 5%, and (c) 10%.

4. Discussion

4.1. Applicability of one-dimensional advection–dispersion analytical solution

The applicability of a one-dimensional ADE is discussed. For the sorption phase, in terms of the breakthrough point ($C/C_0 = 0.05$), the predictions show much

higher pore volumes than the experiment, as shown in Fig. 6. The breakthrough point may be difficult to predict using the one-dimensional ADE when silica sand amended with this MgO agent is used as the attenuation layer material because the relatively slow chemical reaction, namely, the fluoride incorporation into the MgO, is not considered in the ADE. Additionally, the hydration kinetics of this agent is relatively slow, as shown in Fig. 5(a). The MgO
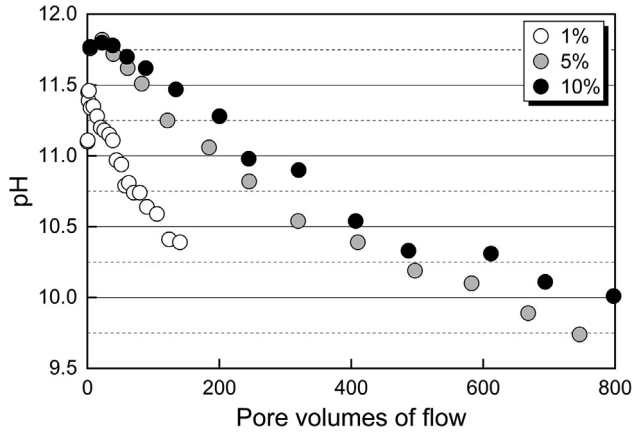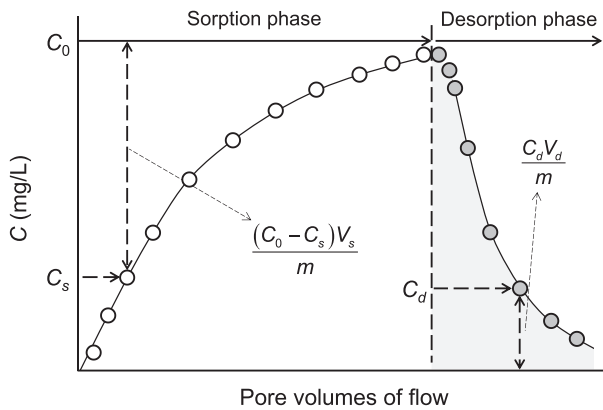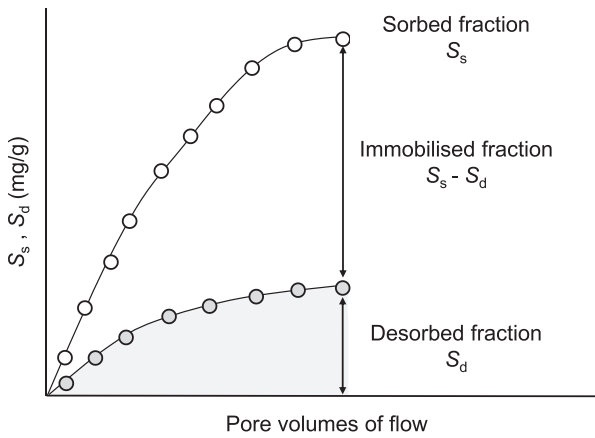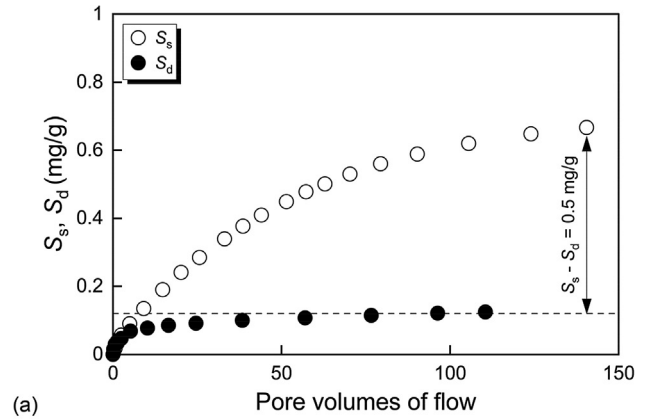
Fig. 7. Profile of the effluent pH during sorption phase.

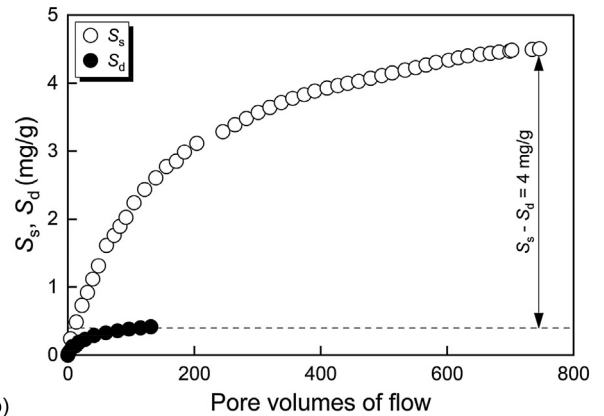(a) Effluent concentration in the sorption–desorption column test

(b) Concept to obtain immobilised fraction

Fig. 8. Conceptual method to estimate the immobilised fraction from the sorption-desorption column test.

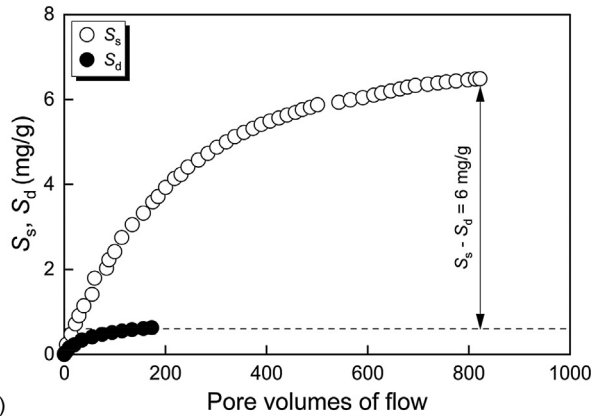Fig. 9. Profiles of S_s and S_d for (a) 1%, (b) 5%, and (c) 10% agent content.

peaks are still detected after 110 days, as shown in Fig. 5 (b), and the incorporation occurred throughout the entire column sorption-desorption test. The prediction agrees well with the experimental results (Igarashi and Shimogaki, 1998). The previous study attributed the main reaction mechanism to reactions such as the ion exchange.

However, an improved analytical method is required for the solute transport on the MgO agent since limitations exist in the ADE when analysing the sorption behaviour using MgO, particularly in terms of the following two issues. First of all, the transformation of MgO to Mg(OH)$_2$ was not taken into account in the aforementioned analysis. Incorporating the sink-source terms and the time-dependent sorption behaviour into the ADE may be considered, such as is shown in the work conducted by Wang and Liu (2005) on the migration of selenium on calcareous soils. Second of all, the pH-dependent behaviour of K_d was not taken into account in the analysis presented here. The electrostatic attraction, dependent on the pH and

other indices, may be included in the analysis to consider such pH-dependent behaviour.

4.2. Evaluation of attenuation layer based on sorption–desorption column test

Fig. 9 shows that the immobilised fraction can be determined using the sorption-desorption column tests. The mechanisms of the ion exchanges by $Mg(OH)_2$ are distinguished between 1) ligand exchange (inner sphere complexes) and 2) electrostatic interaction (outer-sphere complexes) (Morimoto et al., 2009). The chemical interaction of the ligand exchange is stronger than that of the electrostatic interaction. Although these sorption mechanisms are challenging to definitively distinguish, the general trend of the immobilised fraction or the desorbed fraction can be understood through sorption-desorption column tests. When silica sand amended with the stabilising agent of MgO is applied as the attenuation layer material, the sorption and desorption parameters estimated using the analytical solution of the one-dimensional ADE may provide unrealistic values. In such a case, the concept using the immobilised fraction, S_s - S_d, may be a suitable index for evaluating the attenuation layer instead of a solute transport analysis.

A simple evaluation using S_s - S_d under the assumed conditions is discussed. Whether an agent content of 5% is sufficient for use as an attenuation layer material is considered. For an agent content of 5%, S_s - S_d = 4.0 mg/g should be observed in this sorption–desorption column test. If the attenuation layer has a thickness of 50 and is compacted to achieve ρ_d = 1.4 g/cm^3, and if the leachate concentration, C_0 = 8 mg/L F$^-$, enters the attenuation layer, the required sorbed mass, S (mg/g), for 100 years can be calculated as

$$S = \frac{C_0 V_i}{m} \tag{7}$$

where V_i (= $A \cdot I \cdot t$, in which A = 1 cm^2 is a unit area of the attenuation layer, I = 500 mm/yr is the constant infiltration, and t = 100 years) is the volume of the leachate entering the attenuation layer per unit area, and m (=$\rho_d \cdot A \cdot h$, where h = 50 cm is the thickness of the attenuation layer) is the mass of the attenuation layer material.

The required S is assumed to be 0.57 mg/g. This is lower than the immobilised fraction S_s - S_d = 4.0 mg/g. The constant concentration of 8 mg/L F$^-$ is applied in this calculation, but the concentration is 10 times higher than the commonly reported leached value, which is below the limit in Japan regulated under the SCCL of 0.8 mg/L F$^-$. Ito and Katsumi (2020) reported that the concentration of F$^-$ from excavated materials in Japan rarely exceeds 2–3 mg/L. Judging from this simple assumption, silica sand amended with this stabilising agent may be an effective attenuation layer material against fluoride, even if the smaller agent content of 5% is used.

However, this evaluation has a problem. The MgO agent can immobilize more than 80% of the fluoride, as shown in Fig. 9. However, this value should be examined further. It is well known that fluoride is removed via two molecular mechanisms: (1) the incorporation of fluoride in $Mg(OH)_2$, which grows upon contact with water (Morishita and Wada, 2013; Sasaki et al., 2011), and (2) the ion exchange, which occurs on the external surfaces of formed $Mg(OH)_2$ (Morimoto et al., 2009; Sasaki et al., 2011; Ye et al., 2018; Zhen et al., 2015). In-field, the soil, agent, and water are mixed and the mixture is then spread on the ground to construct the attenuation layer (Mo et al., 2020). Therefore, the attenuation layer materials should remain moist even after construction. This means that the MgO in the attenuation layer materials may be hydrated before it makes contact with the in-field permeated fluoride. In this situation, the sorption performance may be overestimated because the sorption mechanism will not occur by incorporation, but fluoride is considered to be taken up only by the ion exchange at the external surfaces of the agent.

Nishikata et al. (2020) placed this MgO agent in distilled water for a month and conducted batch tests. The sorption performance of this MgO agent was seen to be affected by hydration, while the diminution of the sorbed fluoride mass was suppressed within 40% of that before hydration. In this study, the MgO agent was not immediately hydrated, as seen in Fig. 5(a) and (b). The ion exchange as well as the fluoride incorporation are assumed to occur for at least 110 days, but they should be evaluted for longer periods when considering hydration kinetics. Previous research reported that the leaching of some geogenic contaminants from excavated soils was complete within a relatively short period. That is, L/S < 1 (Naka et al., 2016). An important function of the attenuation layer is to immobilise the contaminants at an early stage. Considering these issues, this MgO agent holds promise as an attenuation layer material, but further studies will be necessary to confirm it.

The immobilised fraction can be an index for evaluating the sorption performance of the attenuation layer, while the fraction due to incorporation by hydration should be carefully examined. To consider the on-site conditions, future studies should include an investigation of sorption-desorption column tests cured for several different periods using specimens mixed with soils, agents, and water.

5. Conclusions

This study evaluated the sorption performance of clean sandy soil amended with a stabilising agent for use as an attenuation layer material by means of sorption-desorption column tests. Fluoride was selected as the geogenic chemical, and MgO was used as the stabilising agent. The results support the following conclusions:

(1) In the column sorption tests, breakthroughs ($C/C_0 > 0.05$) occurred after approximately 1, 20, and 50 PVF when the agent contents were 1, 5, and 10%, respectively. Hence, increasing the agent content was seen to delay the breakthrough.

(2) A one-dimensional ADE was employed to model the breakthrough curves from the tests. Using an agent content of 10% produced a partition coefficient, $K_d = 50$ L/kg, but the predictions produced unrealistic estimates for the breakthrough point ($C/C_0 = 0.05$). Giving consideration to the chemical reaction, which depends on time, should improve the solute transport model.

(3) For an agent content of 1% MgO, the percentage of sorbed fluoride mass, S_s, which was desorbed was approximately 20%. The percentage of desorbed mass was much smaller for higher agent contents.

(4) Sorption-desorption column tests were used to determine the immobilised fraction, S_s - S_d. When an 80-mg/L fluoride solution was used as the influent in the sorption phase and distilled water was used in the desorption phase, S_s - S_d = 4.0 mg/g with an agent content of 5% MgO.

(5) According to the XRD patterns, the hydration kinetics of this stabilising agent was relatively slow. Peaks of MgO were still observed after 110 days from the start of the column test. These results suggest that both ion exchange and fluoride incorporation, due to the hydration of MgO, occurred during the column experiments. Future work on the attenuation layer should include a sorption performance evaluation, considering the hydration of MgO.

Acknowledgments

References

Chen, N., Zhang, Z., Feng, C., Li, M., Chen, R., Sugiura, N., 2011. Investigations on the batch and fixed-bed column performance of fluoride adsorption by Kanuma mud. Desalination 268, 76–82. https://doi.org/10.1016/j.desal.2010.09.053.

Grathwohl, P., Susset, B., 2009. Comparison of percolation to batch and sequential leaching tests: theory and data. Waste Manage. 29, 2681–2688. https://doi.org/10.1016/j.wasman.2009.05.016.

Igarashi, T., Shimogaki, H., 1998. Migration characteristics of boron by batch and column methods. J. Groundwater Hydrol. 40, 121–132. https://doi.org/10.5917/jagh1987.40.121 (in Japanese).

ISO 21268-3, 2019. Soil Quality—Leaching Procedures for Subsequent Chemical and Ecotoxicological Testing of Soil and Soil Materials—Part 3: Up-Flow Percolation Test. International Standardization Organization.

Inui, T., Katayama, M., Katsumi, T., Takai, A., Kamon, M., 2014. Evaluating the long-term leaching characteristics of heavy metals in excavated rocks. J. Soc. Mater. Sci., Japan 63, 73–78. https://doi.org/10.2472/jsms.63.73 (in Japanese).

Ito, H., Katsumi, T., 2020. Leaching characteristics of naturally derived toxic elements from soils in the western Osaka area: considerations from the analytical results under the Soil Contamination Countermeasures Act. Japanese Geotech. J. 15 (1), 119–130. https://doi.org/10.3208/jgs.15.119 (in Japanese).

JIS A 1204, 2009. Test Method for Particle Size Distribution of Soils. Japanese Standards Association.

JIS A 1202, 2009. Test Method for Density of Soil Particles. Japanese Standards Association.

JIS R 5201, 2015. Physical Testing Methods for Cement. Japanese Standards Association.

Katsumi, T., 2015. Soil excavation and reclamation in civil engineering: environmental aspects. Soil Sci. Plant Nutrition 61, 22–29. https://doi.org/10.1080/00380768.2015.1020506.

Katsumi, T., Inui, T., Yasutaka, T., Takai, A., 2019. Towards sustainable soil management—reuse of excavated soils with natural contamination. In: Zhan, L. et al. (Eds.), Proceedings of the 8th International Congress on Environmental Geotechnics, Hangzhou, China, vol. 1. Springer, pp. 99–118. https://doi.org/10.1007/978-981-13-2221-1_5.

Magnusson, S., Johansson, M., Frosth, S., Lundberg, K., 2019. Coordinating soil and rock material in urban construction—scenario analysis of material flows and greenhouse gas emissions. J. Cleaner Prod. 241. https://doi.org/10.1016/j.jclepro.2019.118236 118236.

Martínez-Lladó, X., Valderrama, C.M., Rovira, Martí, V., Giménez, J., De Pablo, J., 2011. Sorption and mobility of Sb(V) in calcareous soils of Catalonia (NE Spain): batch and column experiments. Geoderma 160, 468–476. https://doi.org/10.1016/j.geoderma.2010.10.017.

Ministry of Land, Infrastructure, and Transport, Japan, 2010. Technical Manual on the Countermeasure Against Soils and Rocks Containing Naturally Occurring Heavy Metals in Construction Works (Draft). http://www.mlit.go.jp/sogoseisaku/region/recycle/recyclehou/manual/index.htm (accessed 1 June 2020) (in Japanese).

Mo, J., Flores, G., Inui, T., Katsumi, T., 2020. Hydraulic and sorption performances of soil amended with calcium-magnesium composite powder against natural contamination of arsenic. Soils Found. 60 (5), 1084–1096. https://doi.org/10.1016/j.sandf.2020.05.007.

Morimoto, K., Sato, T., Yoneda, T., 2009. Complexation reactions of oxyanions on brucite surfaces. J. Clay Sci. Soc. Japan 48, 9–17.

Morishita, T., Wada, S., 2013. Hydration reaction of magnesium oxide in soil. In: Proceedings of the 48th Symposium on Japanese Geotechnical Society, Kyoto, Japan (in Japanese).

Naka, A., Yasutaka, T., Sakanakura, H., Kalbe, U., Watanabe, Y., Inoba, S., Takeo, M., Inui, T., Katsumi, T., Fujikawa, T., Sato, K., Higashino, K., Someya, M., 2016. Column percolation test for contaminated soils: key factors for standardization. J. Hazard. Mater. 320, 326–340. https://doi.org/10.1016/j.jhazmat.2016.08.046.

Nishikata, M., Yasutaka, T., Morimoto, K., Imoto, Y., Tsukimura, K., 2020. Evaluation of the effect of contact with water on the adsorption characteristics of adsorption materials for an adsorption layer method of construction. In: Proceedings of the 55th Symposium on Japanese Geotechnical Society, Kyoto, Japan (in Japanese).

Nozaki, F., Shimizu, Y., Ito, K., 2013a. Discussion on construction method of heavy metals adsorption layer. In: Proceedings of the 19th Symposium on Groundwater and Soil Contamination and Countermeasures, Kyoto, Japan (in Japanese).

Nozaki, T., Matsuyama, Y., Sugiyama, A., Moriya, M., Komukai, Y., Nagase, T., 2013b. Fundamental study of soil materials for absorbent construction method using MgO material. In: Proceedings of the 19th Symposium on Groundwater and Soil Contamination and Countermeasures, Kyoto, Japan. (in Japanese).

Parks, G.A., 1965. The Isoelectric points of solid oxides, solid hydroxides, and aqueous hydroxo complex systems. Chem. Rev. 65, 177–198. https://doi.org/10.1021/cr60234a002.

Plassard, F., Winiarski, T., Petit-Ramel, M., 2000. Retention and distribution of three heavy metals in a carbonated soil: comparison between batch and unsaturated column studies. J. Hazard. Contam-

inant Hydrol. 42, 99–111. https://doi.org/10.1016/S0169-7722(99)00101-1.

Sasaki, K., Fukumoto, N., Moriyama, S., Hirajima, T., 2011. Sorption characteristics of fluoride on to magnesium oxide-rich phases calcined at different temperatures. J. Hazard. Mater. 191, 240–248. https://doi.org/10.1016/j.jhazmat.2011.04.071.

Tabelin, C.B., Igarashi, T., Villacorte-Tabelin, M., Park, I., Opiso, E.M., Ito, M., Hiroyoshi, N., 2018. Arsenic, selenium, boron, lead, cadmium, copper, and zinc in naturally contaminated rocks: a review of their sources, modes of enrichment, mechanisms of release, and mitigation strategies. Sci. Total Environ. 645, 1522–1553. https://doi.org/10.1016/j.scitotenv.2018.07.103.

Tabelin, C.B., Igarashi, T., Yoneda, T., Tamamura, S., 2013. Utilization of natural and artificial adsorbents in the mitigation of arsenic leached from hydrothermally altered rock. Eng. Geol. 156, 58–67. https://doi.org/10.1016/j.enggeo.2013.02.001.

Tamoto, S., Tabelin, C.B., Igarashi, T., Ito, M., Hiroyoshi, N., 2015. Short and long term release mechanisms of arsenic, selenium and boron from a tunnel-excavated sedimentary rock under in situ conditions. J. Contam. Hydrol. 175–176, 60–71. https://doi.org/10.1016/j.jconhyd.2015.01.003.

Tatsuhara, T., Arima, T., Igarashi, T., Tabelin, C.B., 2012. Combined neutralization–adsorption system for the disposal of hydrothermally altered excavated rock producing acidic leachate with hazardous elements. Eng. Geol. 139, 76–84. https://doi.org/10.1016/j.enggeo.2012.04.006.

Tatsuhara, T., Jikihara, S., Tatsumi, T., Igarashi, T., 2015. Effects of the layout of adsorption layer on immobilizing arsenic leached from excavated rocks. Japanese Geotech. J. 10 (4), 635–640. https://doi.org/10.3208/jgs.10.635 (in Japanese).

Tor, A., Danaoglua, N., Arslan, G., Cengeloglu, Y., 2009. Removal of fluoride from water by using granular red mud: Batch and column studies. J. Hazard. Mater. 164, 271–278. https://doi.org/10.1016/j.jhazmat.2008.08.011.

van Genuchten, M.Th., Parker, J.C., 1984. Boundary conditions for displacement experiments through short laboratory columns. Soil Sci. Soc. Am. J. 48, 703–708. https://doi.org/10.2136/sssaj1984.03615995004800040002x.

Wang, X., Liu, X., 2005. Sorption and desorption of radioselenium on calcareous soil and its solid components studied by batch and column experiments. Appl. Radiat. Isot. 62, 1–9. https://doi.org/10.1016/j.apradiso.2004.05.081.

Wada, S., Morishita, T., 2013. Stabilization of heavy metals contaminated soils by magnesium oxide and related chemical and mineralogical reactions. J. Clay Sci. Soc. Japan 51, 107–117.

Ye, Y., Yang, J., Jiang, W., Kang, J., Hu, Y., Ngo, H.H., Guo, W., Liu, Y., 2018. Fluoride removal from water using a magnesia-pullulan composite in a continuous fixed-bed column. J. Environ. Manage. 206, 929–937. https://doi.org/10.1016/j.jenvman.2017.11.081.

Zhen, J., Jia, Y., Luo, T., Kong, L.T., Sun, B., Shen, W.M.F.L., Liu, J.H., 2015. Efficient removal of fluoride by hierarchical MgO microspheres: Performance and mechanism study. Appl. Surf. Sci. 357, 1080–1088. https://doi.org/10.1016/j.apsusc.2015.09.127.